Structure *14*, 1411–1423, September 2006 DOI 10.1016/j.str.2006.07.006

Mechanism of Gating and Ion Conductivity of a Possible Tetrameric Pore in Aquaporin-1

Jin Yu,[1] Andrea J. Yool,[2] Klaus Schulten,[1] and Emad Tajkhorshid[1,*]
[1] Theoretical and Computational Biophysics Group
Beckman Institute
University of Illinois at Urbana-Champaign
405 N. Mathews Ave.
Urbana, Illinois 61801
[2] Department of Physiology
Department of Pharmacology
Program in Neuroscience
University of Arizona
Tucson, Arizona 85724

Summary

While substrate permeation through monomeric pores of aquaporins is well characterized, little is known about the possible tetrameric pore. AQP1 has been suggested to function as an ion channel upon cGMP activation, although this idea has been controversial. Taking a theoretical and experimental approach, we demonstrate that the current might arise through the tetrameric pore and propose a plausible mechanism for conduction and gating. In response to simulated ion permeation, immediate hydration of the putative central pore was facilitated by moderate conformational changes of pore-lining residues. cGMP is found to interact with an unusually arginine-rich, cytoplasmic loop (loop D) facilitating its outward motion, which is hypothesized to trigger the opening of a cytoplasmic gate. Physiological analyses of wild-type AQP1 and a designed mutant in which two arginines of the gating loop are replaced by alanine provide experimental support for identifying a key component of the proposed mechanism.

Introduction

Aquaporins (AQPs) are members of a family of selective membrane channels abundantly present in all domains of life (Agre et al., 1998; Borgnia et al., 1999; Heymann and Engel, 1999). They are generally known for endowing a high transmembrane permeability to water (Agre, 2004; Preston and Agre, 1991). However, their involvement in diverse cellular functions, including permeation of small molecules other than water (Agre et al., 2002), as well as cell-cell communication (Bok et al., 1982), has been suggested. Aquaporin-1 (AQP1) was the first member of the family to be functionally characterized as a water channel (King and Arge, 1996; Preston et al., 1992). As is predicted for other AQPs, it forms homotetramers (see Figure 1) in cellular membranes (Heymann et al., 1998; Heymann and Engel, 1999; Murata et al., 2000) with each monomer essentially functioning as an independent water pore (de Groot et al., 2001; Tajkhorshid et al., 2002).

*Correspondence: emad@life.uiuc.edu

AQPs are exceptional among membrane proteins with respect to the abundance of atomic resolution structural information that is available. The structure of mammalian AQP1 (Murata et al., 2000; Sui et al., 2001) and AQP0 (Gonen et al., 2005, 2004; Harries et al., 2004), bacterial GlpF (Fu et al., 2000; Tajkhorshid et al., 2002) and AqpZ (Savage et al., 2003), archaeal AqpM (Lee et al., 2005), and plant spPIP2 (Törnroth-Horsefield et al., 2006) have been solved at high resolutions, and the structures of several other AQPs are expected to be available soon. These structures in combination with the numerous theoretical studies (de Groot and Grubmüller, 2001; Grayson et al., 2003; Jensen et al., 2001, 2003; Tajkhorshid et al., 2002; Wang et al., 2005; Zhu et al., 2001, 2004) have provided a detailed picture of the mechanisms of substrate permeation and selectivity of intrasubunit water pores in AQPs. One particularly intriguing property of AQPs is their ability to exclude protons (Pohl et al., 2001; Saparov et al., 2005) while allowing water to pass, a problem that has attracted much attention from theoreticians (Chakrabarti et al., 2004; de Groot et al., 2003; Ilan et al., 2004; Jensen et al., 2003; Tajkhorshid et al., 2002). In contrast, the role of the putative tetrameric central pore (Figure 1) remains poorly understood. Tetramerization is an essential feature of AQPs. The observation that the four monomers each have a functionally independent pore of water, but require a tetrameric organization for function, could suggest a synergistic benefit of oligomerization and, thus, compel further analysis of the potential role of the central pore in AQPs.

A subset of AQP channels including AQP1 have been found to function as ion channels (Saparov et al., 2001; Yool and Stamer, 2002; Yool and Weinstein, 2002). However, the endogenous mechanisms regulating activation remains to be understood. Furthermore, physiological relevance for ion-channel function of AQPs has not been well established yet; only a recent study (Boassa, et al., 2006) has reported physiological significance for AQP1-mediated ion conduction in chroid plexus. Prior work has shown that AQP1 channels can carry nonselective cationic currents after stimulation with protein kinase A (Yool et al., 1996) or by increased intracellular cGMP but not cAMP (Anthony et al., 2000). Curiously, a comparison of the total water and ion fluxes, referenced to unitary conductance values for each, showed that the large ionic conductance response (typically 2–10 μA) seen in *Xenopus* oocytes was carried by only a minor proportion of total water channels present in the membrane (Yool and Weinstein, 2002). Ion substitution experiments and analyses of reversal potentials demonstrated that the current response is associated with a nonselective cation conductance, having approximately equal permeability to Na^+, K^+, and Cs^+, lower but measurable permeability to tetraethylammonium ion, and no appreciable Cl^- permeability (Yool et al., 1996). When purified AQP1 protein was reconstituted in lipid bilayers, a cGMP-dependent cationic channel function was observed, which depended on an intact AQP1 carboxyl terminal domain and was not activated

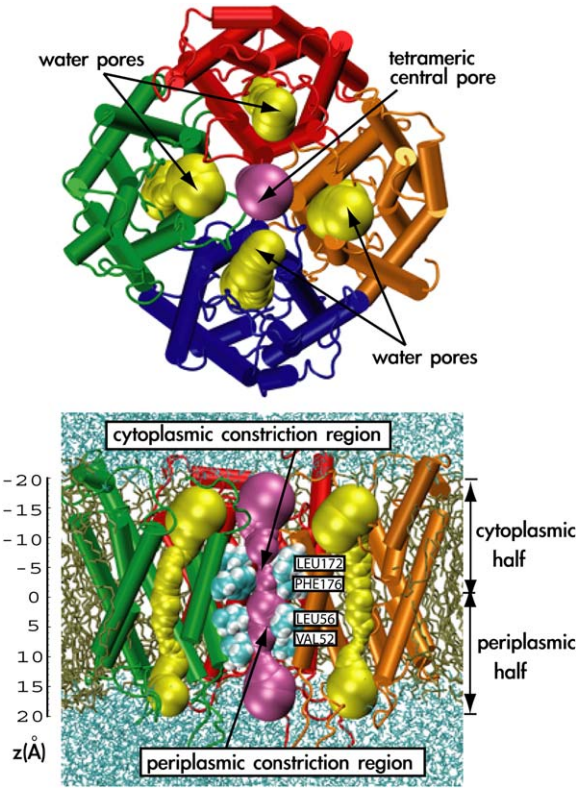

Figure 1. Tetrameric Architecture of AQP1

Cytoplasmic (top) and side (bottom) views of the simulated AQP1 tetramer in lipid bilayer and water. Water and lipid were removed to create the view in the top panel. The four AQP1 monomers are shown in different colors. Water is known to move through the individual water pores formed by the monomers, while the tetrameric central pore has been proposed to function as a nucleotide-gated ion channel. The tetramer was imbedded in a POPE lipid bilayer (dark green stick representation) and solvated by water (light blue stick representation) on both sides of the membrane. In the side view (lower panel), the front monomer is removed for clarity. Side chains of residues lining the cytoplasmic and periplasmic constriction regions of the central pore, respectively, (VAL52, LEU56, LEU172, and PHE176 in the bovine AQP1 sequence) are shown in van der Waals (VDW) representation. The size of the central pore and the water pores are depicted with the channel radius profile calculated by the program HOLE (Smart et al., 1996), purple for the central pore and yellow for the water pores. The tetramer is aligned along the z axis in the present study, as shown in the bottom view.

by cAMP; however, it is important to note that the fraction of water channels that were available to function as gated ion channels in the bilayer was even lower than that seen in oocytes, approaching one per million and prompting the speculation that AQP1 ion channel function is an accident of protein misfolding (Saparov et al., 2001). This low open channel probability called into question the possible functional relevance of the ion channel, yet mutagenesis studies suggested the ionic conductance depended on conserved sequence domains in AQP1. Regions of the AQP1 molecule (such as the carboxyl terminal domain) are highly conserved in amino acid sequence in AQP1 proteins across species yet apparently are not essential for the water-channel function (Zeidel et al., 1994). When key carboxyl terminal residues are altered by site-directed mutagenesis, the AQP1 ionic current activation is impaired, but water permeability is retained (Boassa and Yool, 2003). Amino acid sequence conservation in structures that are apparently not needed for water-channel function can be deduced to confer some other functional advantage. The C-terminal sequence of AQP1 shows some interesting though incomplete similarities with the sequences of other cGMP binding proteins (Boassa and Yool, 2002). Binding studies characterized a low affinity binding site for cGMP in AQP1-expressing membranes, and electrophysiological data provided a pharmacological profile for AQP1 ion-channel activation and inhibition that was consistent with that of other cGMP-gated ion channels (Anthony et al., 2000). Recent work characterizing AQP1 channels natively expressed in choroid plexus has confirmed the gated ion channel function and provided evidence for a physiologically relevant contribution to the regulation of cerebral spinal fluid production (Boassa et al., 2006). Further support for the concept that AQPs can function as ion channels comes from other work showing that the pH-sensitive AQP6 (Liu et al., 2005; Yasui et al., 1999) and the tyrosine-kinase-sensitive *Drosophila* aquaporin-related protein BIB (big brain) (Yanochko and Yool, 2002, 2004) function as ion channels showing properties of total membrane conductance amplitudes and voltage independence similar to that of AQP1 when expressed in oocytes but with contrasting mechanisms of activation and different ionic selectivities (AQP1 and BIB are cationic; AQP6 is anionic). These differences rule out the alternative hypothesis of a ubiquitous endogenous oocyte current.

Part of the uncertainty regarding the ion-channel function of AQP1 has stemmed from the fact that single channel properties and responsiveness to intracellular cGMP can vary with the expression system. For example, in oocytes, batch-to-batch variability in the amplitude of the AQP1 ionic current response to forskolin has been observed by our lab and others, a complication that has been suggested post hoc to have arisen in part from crosstalk between complex intracellular signaling systems in the oocyte system and perhaps from interactions with yet-unidentified accessory proteins (Yool and Stamer, 2002). Expression system specific differences in AQP1 ion-channel function are clear: when reconstituted in bilayers, purified AQP1 protein showed a reduced unitary conductance and a substantially lower open probability (Saparov et al., 2001) as compared with AQP1 channels in oocytes. In transfected AQP1-expressing HEK cells, no ion-channel currents were measured in response to cGMP (Tsunoda et al., 2004). In contrast, native AQP1 channels in choroid plexus show a robust ion channel conductance in response to cGMP that is lost after AQP1 knockdown by small interfering RNAs (Boassa et al., 2006). Pancreatic secretory granules generate a cationic conductance response to cGMP that depends on AQP1 coassembly with other members of a protein-signaling complex (Abu-Hamdah et al., 2004). The possibility that AQP1 ion-channel gating depends on convergent processes of signaling and protein-protein interactions is consistent with all the data currently available.

Identification of Mg^{2+} binding sites at the 4-fold symmetry axis of the tetramer of GlpF (Fu et al., 2000), another member of the AQP family, supports the notion of ion flux through the central pore. The tetrameric

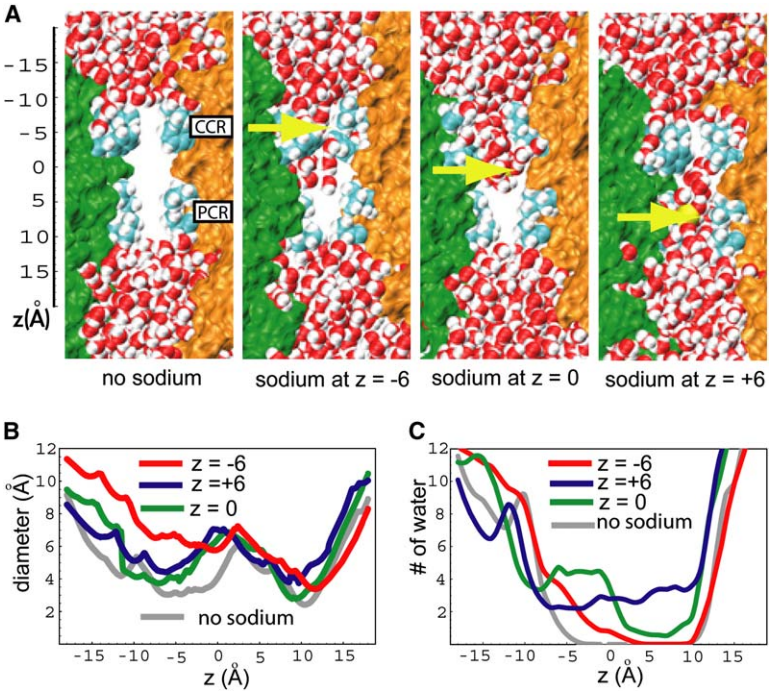

Figure 2. Variations of Dimension and Extent of Hydration of the Central Pore in Response to the Presence of a Permeating Ion

(A) Snapshot views from simulations show a side view of the central pore in the absence (closed) and presence of a sodium ion at varying positions along the z axis. Water molecules are shown as VDW spheres. Side chains of residues lining the cytoplasmic (CCR) and periplasmic constriction (PCR) regions are shown in VDW representation. The position of the sodium ion (yellow sphere) is highlighted by yellow arrows. In unperturbed (closed) AQP1, water molecules are precluded from the core region by the CCR and PCR, leaving the central pore dry. Significant hydration of the central pore can be obtained after introducing an ion into the channel at different positions.

(B) Diameter profile calculated by the program HOLE (Smart et al., 1996) along the central pore for different simulations.

(C) Water occupancy along the pore axis, calculated as the number of water molecules in 1 Å thick cylindrical slabs (within ~9 Å of the pore axis) and averaged over the duration of each simulation.

arrangement of AQP1 is reminiscent in overall structural organization of that of ion channels such as the K^+ and cyclic nucleotide-gated channels (Jan and Jan, 1992; Zagotta and Siegelbaum, 1996), which feature a central pore as a gated pathway for ions.

In the field of aquaporins, further work is essential for clarifying the mechanisms of regulation and the physiological roles of dual water and ion-channel capabilities. The purpose of the work here is not necessarily to resolve any remaining elements of the controversy but to test whether ion permeation is theoretically possible, taking advantage of the known crystal structure of AQP1 and the power of molecular dynamics simulations to calculate barriers against ion movement through intrasubunit water pores and the unknown potential of the central pore as a candidate ion conducting pathway. Differences in pharmacological sensitivities of the ionic and water permeabilities of AQP1 suggested that these permeation pathways within the tetrameric molecule are structurally distinct (Saparov et al., 2001; Yool et al., 2002), thus raising the possibility that the central axis of 4-fold symmetry might be a candidate pathway for ion flux (Boassa and Yool, 2002; Fu et al., 2000; Yool and Weinstein, 2002). These results generate testable predictions for future work.

We probed through molecular dynamics simulations the central pore as a putative pathway for cGMP-induced ionic currents as suggested by experiments. We have studied structure and dynamics of the central pore through a comprehensive examination of its size and hydration, incorporating analyses of conformation and hydrophobicity of residues lining the central pore. Unexpected insights were found for conformational coupling of pore-lining residues with movement of other parts of the protein, especially in a conserved cytoplasmic loop region where cGMP appears to interact. By constraining a candidate permeant ion at different levels along the pore axis and simulating ion conduction events, we have identified potential locations and nature of energy barriers against ion permeation in the closed state. Simulations offer insights into how an ion might permeate the activated channel, the range of protein conformational changes needed to accommodate ion permeation, whether such changes can be tolerated by the protein, and to what extent the central pore needs to be physically expanded to accommodate a permeating ion with its first hydration shell.

In parallel, simulations investigating the binding of cGMP to the cytoplasmic side of the protein predicted a possible mechanism for the coupling of cGMP binding to the cytoplasmic face of AQP1 and conformational changes in the cytoplasmic half of the central pore that initiate the opening of the pore. Our data suggested that gating of the central pore is mediated at least in part through cGMP-induced conformational changes of one of the cytoplasmic loops (loop D), which is spatially juxtapositioned with two hydrophobic residues forming the putative cytoplasmic gate of the central pore. The involvement of this cytoplasmic loop in the gating process was successfully verified by mutational experiments showing that substitution of two key arginines from the loop resulted in an almost complete removal of the nucleotide-activated ion conduction with no appreciable effect on the water permeability.

Results

Nature of Permeation Barriers in the Closed State

For clarity, the cavity at the 4-fold symmetry axis, which has been proposed as a candidate structure for the observed gated ion conductance in AQP1, is referred to here as the "central pore." The diameter profile of the central pore of AQP1, calculated by the program HOLE (Smart et al., 1996) at the end of the 3 ns unperturbed equilibration is shown in Figure 2. The central pore region can be defined as a 30 Å membrane spanning

region (from z = −15 Å to z = 15 Å) (Figures 1 and 2). For crystal structures obtained in the absence of cGMP, the central pore is presumed to be closed. In this state, the central pore can be characterized by two major constriction regions: one with a diameter of about 3.1 Å in the cytoplasmic half, formed by side chains of LEU172 and PHE176 (cytoplasmic constriction region, CCR), and the other with a diameter of about 2.4 Å in the periplasmic half of the channel, lined by side chains of VAL52 and LEU56 (periplasmic constriction region, PCR) (Figure 2). All the amino acids lining the two constriction regions are hydrophobic. In our equilibration simulations, the CCR and the PCR effectively keep water molecules from entering the central pore, thus acting as gatekeepers in creating a dehydrated cavity (about 20 Å long) spanning the region between CCR and PCR (see Figure 2A).

The central pore is mainly lined with hydrophobic side chains. Therefore, a permeating ion would have to be accompanied by its first hydration shell as there are no polar/charged residues that would be expected to compensate for the desolvation energy cost. While certain regions of the central pore are large enough in the closed state to accommodate a hydrated ion, in the two major constriction regions, spatial constraints are unlikely to allow an ion to pass along with its hydration shell. Therefore, we would expect that any reasonable gating mechanism would have to trigger conformational changes in these regions that would allow water molecules to penetrate and fully hydrate the central pore in advance of ion conduction.

Simulations with a sodium ion constrained at different sites inside the pore were performed to investigate the extent of conformational changes within the central pore that could arise in response to ion permeation. The simulations lasted each about 10 ns, a timescale comparable to that of a cation passing through the gated channel as estimated from experiments (Anthony et al., 2000) measuring a 150 pS conductivity at a driving force of ~100 mV.

After placement of a sodium ion in the middle of the central pore (z ~ 0 Å), water molecules from the cytoplasmic side quickly penetrated the CCR and filled the cytoplasmic half within 100 ps. Further penetration of water into the periplasmic half of the channel was prevented by side chains of LEU56, thus leaving the PCR dehydrated for most part of the simulations. The diameter profile and hydration pattern of the partially hydrated pore observed at the end of the simulation are shown in Figures 2B and 2C, respectively. The diameter profile indicated that the presence of an ion in the middle of the pore results in a larger expansion of the cytoplasmic side as compared with the periplasmic side. Visual examination of the trajectories suggests that the observed expansion is correlated to intrusion of water, which penetrates more rapidly from the cytoplasmic side, indicating that the CCR is more flexible than the PCR.

Upon constraining a sodium ion at the CCR (z ~ −6 Å), the partially hydrated ion rapidly recruited several water molecules from the cytoplasmic side and became fully hydrated. Soon after, the cytoplasmic half of the pore was partially hydrated. However, water molecules were stopped at the PCR by side chains of LEU56. It seems that this side chain constitutes to a key barrier

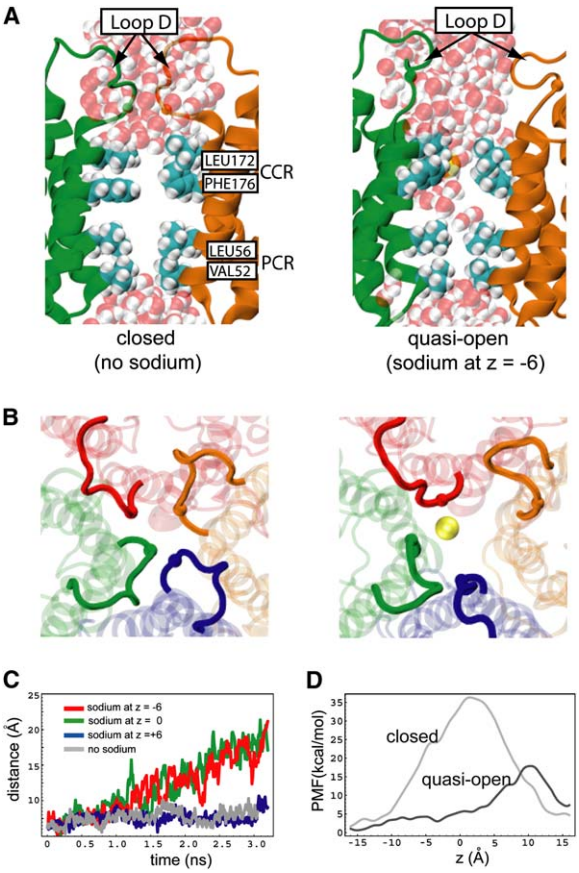

Figure 3. Partial Opening of the Central Pore in Response to Occupancy by an Ion

Views of the cytoplasmic loops D in AQP1 are shown in snapshots from simulations after 3 ns equilibration of the unperturbed AQP1 (closed state, left panels) and after 10 ns simulation of AQP1 with a sodium ion (yellow sphere) constrained at the CCR (quasiopen, right panels). (A) Side view of the central pore. Water molecules are shown in VDW representation. Residues LEU172 and PHE176 at the CCR and VAL52 and LEU56 at the PCR, as well as water are shown in VDW representation. (B) View of the central pore from the cytoplasmic side. On each loop D the position of the C_α atom of GLY168 is highlighted as a small sphere and was used to measure the separation of the loops induced by the presence of Na^+ in the pore. (C) Separation of the cytoplasmic loops D, calculated as the distance between the C_α atoms of opposing GLY168 residues on the loops D in diagonally opposite subunits, in different simulations. (D) Potential of mean force (PMF) associated with ion permeation through the closed AQP1 and through a "quasiopen" pore, the latter established after 10 ns simulation with a sodium ion at the CCR.

against full hydration of the entire pore, preventing water molecules from penetrating the PCR both from the cytoplasmic and the periplasmic sides. Nevertheless, water molecules from the hydrated cytoplasmic half channel occasionally and transiently populated the PCR during the simulation. An example is captured in the snapshot shown in the right panel of Figure 3A. The diameter profile (Figure 2B) at the end of this simulation indicates an expansion of about 4 Å of the cytoplasmic side of the pore. There is no discernible expansion in the PCR, though, and water molecules entering from the cytoplasmic side seem to only induce slight conformational changes in the PCR.

With a sodium ion constrained at the PCR (z ~6 Å), water molecules were drawn immediately from the periplasmic side into the pore. These water molecules gradually penetrated the pore all the way through to the CCR and joined water molecules on the cytoplasmic side after about 2 ns, thus leading to a hydrated channel. Although the limited timescale of the simulations might not be sufficient for a fully developed response of the protein, comparison of the hydration patterns observed in the two simulations, with an ion positioned at either the PCR or the CCR, suggests again that the presence of an ion inside the pore triggers conformational changes that are larger in the cytoplasmic half than in the periplasmic half of the pore. These observations are consistent with the idea that cytoplasmic events gate the channel.

Gating Role of Cytoplasmic Loops

Since cGMP is a cytoplasmic messenger, its putative binding site and the resulting conformational changes relevant to gating of the AQP1 ion conductance are likely to be initiated by ligand-protein interactions at the cytoplasmic side (Boassa and Yool, 2002). In order to identify regions that might be involved in binding and gating of the central pore, we inspected the cytoplasmic surface of the protein for flexible regions. As expected, no large conformational changes of the transmembrane segments were observed, even after placement of the ion inside the central pore. We did, however, observe concerted large motions of one of the cytoplasmic loops (loop D, residues 161–169 in each monomer of bovine AQP1), a major constituent of the vestibular entrance to the central pore. Together, the four central loops from the four monomers act as a cap that can physically occlude the inner vestibule of the central pore. Shown in Figures 3A and 3B are snapshots taken from simulations of AQP1 with and without an ion constrained at the CCR. A large separation between the D loops was found to accompany the small conformational changes of the CCR. LEU172, located at the CCR, sits at the region linking helix V to loop D (in the unperturbed AQP1, the loop ends at the first turn of the membrane-spanning helix). After a few nanoseconds of simulation with a sodium ion at the CCR, an outward motion of the loop and unwinding of the first turn of helix V were observed. During this process, side chains of LEU172 started to separate from each other, thus leading to a widening of the CCR and allowing water to penetrate. The coupling of the presence of an ion in the CCR and the widening and hydration of the pore appears to be a key element for the gating process. It is well known that the size of hydrophobic constriction sites is an important factor in hydration (Beckstein and Sansom, 2003, 2004; Beckstein et al., 2004). A hydrophobic constriction site can act as an efficient barrier to ion and water permeation if its diameter is less than the diameter of an ion with a first hydration shell (Beckstein and Sansom, 2003, 2004; Beckstein et al., 2004). Preliminary simulations show that removal of the bulky side chains from the two constriction regions results in a rapid hydration of the pore even in the absence of an ion. Interestingly, the calculated diameter of PCR in this mutant is only about 5 Å, yet a full hydration of the central pore is observed in less than 1 ns. The diameter of CCR in the mutant is about 7 Å, which is interestingly the same as the diameter of CCR in our quasiopen state.

The hydration of such narrow regions indicates that pores formed by proteins, which are lined by irregularly shaped and highly fluctuating amino acid side chains, might behave very differently from perfectly cylindrical nanopores used to calibrate minimum radii needed for hydration (Beckstein and Sansom, 2003, 2004; Beckstein et al., 2004).

The concerted outward motion of the loops D, effectively opening the cytoplasmic vestibule of the central pore, can be clearly seen in Figure 3A. In other simulations performed in the presence of a sodium ion, similar motions of the loops were observed. As a measure of separation of the four D loops, we show in Figure 3C the distance between GLY168:Cα atoms from loops D in diagonally positioned subunits. The most significant opening of the inner vestibule, reflected by an increase in the separation between GLY168 residues from 6.5 Å to over 20 Å, was observed in simulations in which an ion was constrained either at the CCR or at the center of the pore. It seems that there is a strong coupling between the widening of the CCR and the outward motions of the D loops.

In addition to the bovine AQP1 crystal structure (Sui et al., 2001) used for models simulated in this study, the crystal structure of human AQP1 has also been solved (Murata et al., 2000). Comparison of structures of human and bovine AQP1 proteins, which are highly conserved in primary sequences, clearly shows that loop D has been captured in two distinct conformations in the two structures (Figure 4A). The conformations could reflect a capacity of loop D to undergo a flipping motion, which is comparable to the outward shift of loop D observed in our simulations. The different conformations of the loop in the structures of bovine and human AQP1 may be merely due to different crystal contacts; however, they might also indicate that D loops are flexible enough to adopt two intrinsically stable conformations under in vivo conditions.

Energetics of Ion Permeation through the Central Pore

In order to study full permeation of an ion through the central pore, we applied the method of steered molecular dynamics (SMD) (Isralewitz et al., 2001) to pull a sodium ion through the central pore and to investigate how it interacts with the protein. This model was used to assess the protein conformational changes and the displacement of water molecules that might accompany an ion permeation event. In all pulling experiments, the permeating ion brought along some additional water molecules while passing through the originally dehydrated pore (~four water molecules within the first hydration shell of the ion).

From the SMD trajectories, we calculated the potential of mean force (PMF), i.e., the free energy profile of ion permeation. The PMF of the unperturbed AQP1 central pore, representing a closed channel, is shown in gray in Figure 3D. A high free energy barrier amounting to over 30 kcal/mol spans the core region of the central pore. The region between the two constriction regions presents a hydrophobic environment that would not favor a permeating ion. The free energy profile shows

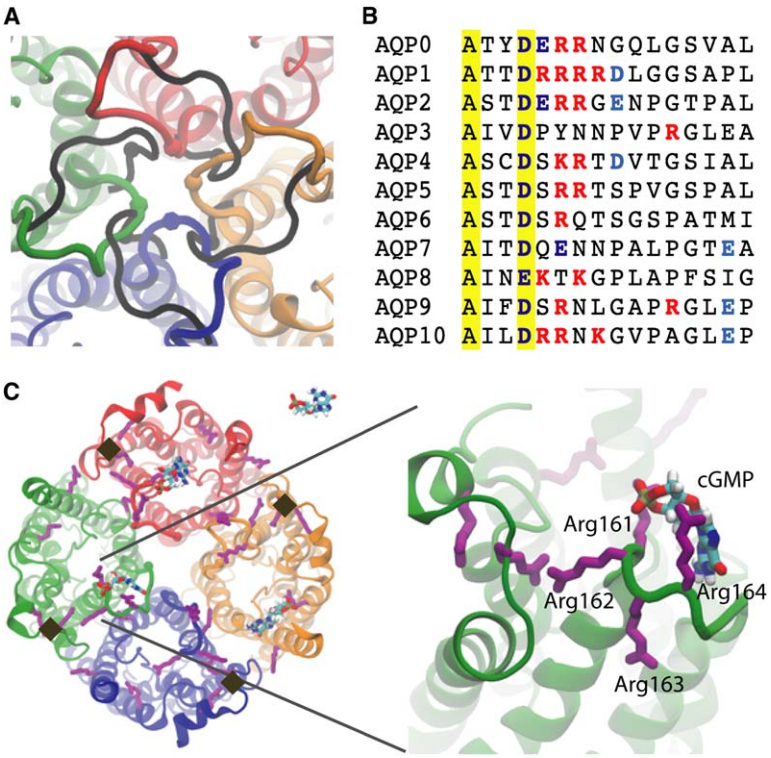

Figure 4. The Proposed Gating Role of Loop D Mediated through Interaction of cGMP with an Arginine Array

(A) Comparison of two different conformations of loop D in the published crystal structures of bovine AQP1 (Sui et al., 2001) (colored) and human AQP1 (Murata et al., 2000) (dark gray).

(B) Sequence alignment of loop D in human AQPs. An extensive polyarginine motif is present only in AQP1.

(C) Binding of cGMPs to loop D shown in a snapshot taken after a 10 ns simulation of AQP1 with four cGMP molecules. The cGMP molecules are colored according to atom types; the initial positions of the nucleotides at the perimeter of the cytoplasmic face of the tetramer are shown with dark diamonds. Arginine residues at the cytoplasmic surface of AQP1 are shown in magenta stick representations. The right panel is a close-up, slightly rotated view showing the interaction of one of the bound cGMP molecules with arginines on loop D.

a broad peak with the maximum at the middle of the transmembrane pore consistent with an absence of any stabilizing interaction for an ion within a dehydrated pore.

As described in the previous section, placement of an ion at the CCR caused water molecules from the cytoplasmic region to enter the pore. Water molecules could not, however, penetrate the PCR and fully hydrate the entire pore, as shown in Figures 2 and 3. Since dehydration introduces a substantial barrier to ion permeation, one predicts that partial hydration of the cytoplasmic half, as visualized at the end of this simulation, should significantly reduce the magnitude of the energy barrier. The more permissive state of the central pore can be considered as a model for a channel in a quasiopen (see the right panel of Figure 3A) state. In order to test whether the ion permeation through this quasiopen channel is energetically different from permeation through the closed channel, the respective PMF was calculated (Figure 3D). The details of SMD simulations are described in Supplemental Data (available with this article online). Results of the simulations showed that in the quasiopen state, the cytoplasmic contribution to the barrier is virtually eliminated, and the residual barrier at the PCR shows an amplitude that is approximately half of that seen for a closed channel. The almost complete removal of the CCR barrier is due to the hydration of this region. In the periplasmic half, on the other hand, the drop of the barrier height is very likely caused by partial penetration of water molecules from the cytoplasmic side (as exemplified by the snapshot shown in the right panel of Figure 3A). Subtle conformational changes of the side chains of LEU56 and VAL52 triggered by water molecules at the PCR would reduce the barrier further. These results support the hypothesis that the gating process involves the opening of two hydrophobic gates, one in each half channel, whose hydration will reduce the energy barrier, thus allowing ions to pass.

In a few test simulations, a sodium ion was placed at different regions of the quasiopen channel but was allowed to move freely after an initial phase of constraint lasting a few picoseconds. An ion placed at z = +10, i.e., in the periplasmic half of the channel, spontaneously went through the channel (in the $-z$ direction) to the cytoplasmic side within 1 ns; an ion placed initially at z = +12 immediately exited the channel to the periplasmic side, i.e., no permeation was observed. The simulations demonstrate that once the ion has crossed the barrier (at $+10 \leq z \leq +12$) of the quasiopen channel, permeation through the rest of the channel can proceed rapidly.

We also performed simulations in which a sodium ion was repeatedly pulled through the central pore, in order to see whether partial hydration of the pore induced by primary ion permeation events could facilitate subsequent permeation events. Profiles of water occupancy and ion trajectories calculated from these simulations are provided in Supplemental Data.

cGMP Binding and the Gating Mechanism

In order to investigate the effects of the reported channel-activating ligand, cGMP, at the cytoplasmic face of AQP1, we performed simulations in which four cGMP molecules were added near the perimeter of the tetramer, at each of the four C termini of the monomers (Figure 4C). The distal segment of the C terminus (residues 250–269) is missing from the crystal structure of the monomer but does not appear from experimental work to be necessary for the gating of AQP1 ion conductance (Boassa and Yool, 2002).

After about 2 ns in this simulation (Figure 4C), two of the cGMP molecules have diffused from the periphery of the tetramer to the center where they directly interact with the D loops. By simultaneously interacting with multiple amino acids on the cytoplasmic surface, the nucleotide molecules facilitate an outward motion of loop D away from the inner vestibule of the central pore (movies showing these events are provided as Supplemental Data). Compared with the initial conformation of the loops, shown in Figure 4A, the loops moved significantly after the binding of cGMP ligands. The outward motion of the D loops and the apparent binding of the nucleotides were not an enduring effect. The nucleotide position and orientation fluctuated, and an associated transient opening of the cytoplasmic entrance of the pore did not persist enough to induce hydration of the central pore during the 10 ns simulation. However, the two cGMP molecules remained close to their respective loops for the duration of the simulation.

During the simulations, the other two cGMP molecules diffused freely along the cytoplasmic surface of the protein but did not establish any interaction with the D loops during the 10 ns simulation. One cGMP molecule simply diffused away from the tetramer, while the other one stayed at the periphery of the tetramer, near peripheral arginine residues.

Examination of the interactions suggests that cGMP molecules preferentially interact with regions rich in arginine residues. The interaction is consistent with the negative charge of the phosphate group and the hydrogen-bonding capacity of the cyclic nucleotide. A total of seven arginine residues are located on the cytoplasmic surface of each AQP1 monomer, with each loop D carrying four. The arginine-rich loop D shows features consistent with a role in cGMP binding and activation of the central pore channel. Furthermore, it is possible that the nucleotide ligands interact with multiple arginine domains in loop D and the C terminus. Obviously, we are not capturing the entire binding and gating of the central pore in a 10 ns simulation. However, our simulations clearly indicate that cGMP has a strong tendency to interact with arginine-rich regions at the cytoplasmic side of the protein. Combined with binding of cGMP to its specific binding site, which might be located on the periphery of the tetramer, the nonspecific interaction with loop D can result in a large outward motion of the latter. We hypothesize that such conformational changes in turn affect the CCR barrier in the central pore. It is intriguing that within the family of mammalian AQPs, AQP1 is unique in having the most consecutive arginine residues in the loop D sequence (Figure 4B).

Further work is needed to definitively link the proposed binding of cGMP to loop D and the activation of the ion conduction in AQP1. Our simulations indicate that there is an intrinsic affinity between the nucleotides and loop D, especially with the arginine array, and suggest that nucleotide binding might facilitate an outward motion of the loop D, which in turn might enable the expansion of the CCR of the central pore, and subsequent steps of hydration and permeation.

Mutational Studies of the Gating Domain

The results of our simulations suggested that a flexible polyarginine loop (loop D) located at the intracellular face of the putative central pore acts as a candidate "gating" domain at the central pore. This role of loop D was tested by site-directed mutagenesis and biological assays comparing ion-channel and water-channel properties of wild-type human AQP1 and a mutant construct in which two of the arginines were replaced by alanines. These sites, R159 and R160 in human AQP1 used for biological assays, are identical to R161 and R162 in the bovine AQP1 protein used for our simulations.

The substitution of arginines at positions 159 and 160 with alanine (R159A+R160A) had no effect on the measured osmotic water permeability; the hypotonic swelling response of oocytes expressing mutant channels was not significantly different from that with wild-type (Figure 5A). These results indicate that the double mutation does not prevent channels from assembling and targeting the plasma membrane with an efficiency comparable to that of wild-type. However, the net ionic conductance response to increased intracellular cGMP was greatly impaired in the mutant (Figure 5B). The mean conductance of R159A+R160A-expressing oocytes was significantly less than that of the wild-type and not significantly different from control oocytes that did not contain AQP1. Current amplitudes monitored as a function of time (applying repeated brief voltage steps to +40mV at 6 s intervals) illustrate a representative response of wild-type but not mutant channels to sodium nitroprusside (SNP) (Figure 5C). For constructing current-voltage relationships, current traces were measured over a range of voltage steps (−110 to +40 mV, from a holding potential of −40 mV) at the initiation of the recording (time 0) and at 8 min after extracellular application of SNP (Figure 5D). Conductances were calculated from the slope of the current-voltage relationships (Figure 5E). The magnitudes of the ionic conductance responses that were induced by SNP were calculated by subtracting the initial conductance (measured at time zero) from the final conductance (measured 7 min after SNP); these net ionic conductances are summarized for statistical comparison in Figure 5B and illustrate the effective elimination of the current by the double arginine mutation.

Discussion

The interior of the central cavity of AQP1 is quite hydrophobic and cannot provide a permeant ion with any stabilizing interactions. If this region serves as the ion pore of AQP1, an ion can only permeate it without shedding its first hydration shell, as even partial dehydration of the ion would result in a considerable energy cost. In the absence of cGMP, a closed state of the central pore of AQP1 appears to be effectively furnished by steric and hydrophobic barriers against water penetration at the two major constriction regions flanking the cytoplasmic and periplasmic sides of the central pore, thus ensuring a dry cavity. In our model, hydration of the central pore requires widening of the two constriction regions as a prerequisite for ion permeation. Destabilizing either of the constriction regions, as was done in our simulations through artificially inserting an ion into the bottleneck regions, might facilitate the entrance of water molecules into the cavity, hence facilitating ion permeation.

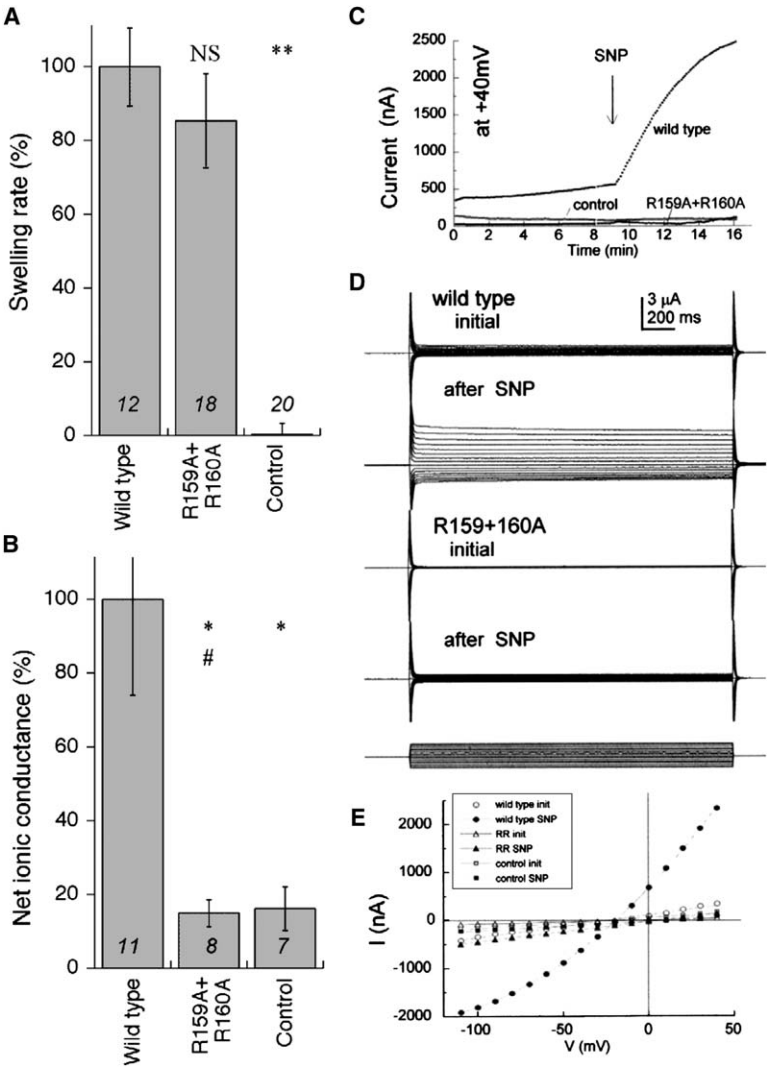

Figure 5. Effects of Mutations of Arginine Residues in the Loop D of AQP1 on Water Permeability and cGMP-Induced Cationic Conductances

(A) Histogram summary of swelling in 50% hypotonic saline, standardized to the mean response of oocytes expressing wild-type AQP1. Wild-type and mutant R159A+R160A AQP1 channels were assembled and expressed in the oocyte membrane with comparable efficiency, as evidenced by osmotic water permeability. Control oocytes showed no discernable osmotic water permeability. Data are mean ± SE; n values are shown in italics.

(B) Histogram summary of net conductances measured from the slope of the current-voltage relationship for currents measured at 8 min after extracellular application of SNP after subtraction of the initial conductance (see text for details). The double arginine mutations significantly impaired the ionic conductance response. Data are mean ± SE; n values are shown in italics. Statistical significance (panels [A] and [B]) was determined by analysis of variance and post-hoc Student's t test for unpaired data with unequal variance. NS, not significantly different from wild-type; double asterisk and asterisk, significantly different from wild-type with $p < 0.005$ and $p < 0.05$, respectively; pound sign, not significantly different from control.

(C–E) Representative ionic currents recorded during before and after application of sodium nitroprusside (SNP: inducing increased intracellular cGMP) in oocytes expressing wild-type and R159A+R160A AQP1 channels and in control oocytes. (C) The activation of the response was monitored with repeated brief (200 ms) steps to +40 mV from holding potential of −40 mV; SNP at a final concentration of 1.6 mM was added at the time indicated (arrow). (D) Currents measured for a range of voltage steps (−110 to +40 mV; holding potential −40 mV) for the same oocytes illustrated in panel (C). (E) Plot of current amplitude as a function of voltage for traces shown in panel (D).

Our simulations revealed that subtle conformational changes of amino acid side chains lining the central pore, especially at the CCR, were sufficient to trigger the hydration of the pore, which removes a major barrier against ion permeation. Selected mutations of amino acids lining the constriction regions of the channel would be predicted to impact the ease of hydration of the pore and might alter the open probability of the channel. Experimental tests of these predictions will be a compelling avenue for future research. Based on the simulation results, the CCR seems to be conformationally more flexible than the PCR, in that placement of an ion anywhere along the central channel axis can easily initiate the hydration of the cytoplasmic half of the channel. This observation is consistent with a gating mechanism that initiates channel opening from the cytoplasmic side, as would be expected in the case of cGMP, which is an intracellular second messenger. We propose that cGMP binding at loop D causes conformational changes at the CCR and serves as at least one of the steps involved in activation of ionic conductance through the putative central pore. Previous studies have shown that wetting of a channel is very sensitive to its radius (Allen et al., 2002; Beckstein and Sansom, 2003, 2004; Beckstein et al., 2004; Sotomayor and Schulten, 2004). Therefore, even a small perturbation and partial opening of the pore at the CCR may bring water into the cavity, as observed in our simulations. The hydration of the cytoplasmic half channel might in turn facilitate the opening of the PCR, as was also observed although transiently, in our simulations; the full hydration of the entire pore could represent an open ion-conducting AQP1 channel.

Results presented here, although limited by the short timescale of the simulations, suggest that permeation of cations through a central pore pathway is theoretically possible in AQP1 and offer new insights into regions that could be involved in the gating of the channel. Deciphering the contributions of hydrophobic barriers within the putative central pore to the properties of ion permeation in AQP1 will be of interest in future studies combining the strengths of theoretical modeling, molecular

Table 1. Alignment of Loop D Residues of AQP1 and Related Proteins

Accession Number	Genus Species	Sequence (aa Number)			Common Name
NP_932766	*Homo sapiens*	156	TT*D**RRRRD*LGGSAP	169	human
NP_999619	*Sus scrofa*	158	TT*D**RRRRD*LGGSAP	171	pig
AAW47637	*Notomys alexis*	117	TT*D**RRRRD*LGGSAP	130	Spinifex hopping mouse
CAA48134	*Rattus norvegicus*	156	TT*D**RRRRD*LGGSAP	169	Norway rat
XP_519026	*Pan troglodytes*	281	TT*D**RRRRD*LGGSAP	294	chimpanzee
AF495880.1	*Oryctolagus cuniculus*	134	TT*D**RRRRD*LGGSAP	147	rabbit
BC007125.1	*Mus musculus*	156	TT*D**RRRRD*LGGSAP	169	house mouse
NM_174702.2	*Bos taurus*	158	TT*D**RRRRD*LGGSGP	171	cow
BAA93428	*Canis familiaris*	158	TT*D**RRRRD*LGGSGP	171	dog
NM_001009194.1	*Ovis aries*	158	TT*D**RRRRRD*LGDSG	171	sheep
AB094502.1	*Anguilla japonica*	159	TT*DKRRRD*VTGSAP	162	Japanese eel
AY817455.1	*Passer domesticus*	158	TT*D**RRRN*DVSGSAP	171	house sparrow
AB073315.1	*Hyla japonica*	161	- T*D**RRRRD*VSGSVP	173	Japanese tree frog
AY692368.1	*Coturnix coturnix*	157	TT*D**RRRN*DVTGSAP	170	common quail
BC075384.1	*Xenopus tropicalis*	164	- T*D**RRRN*DVSGSAP	176	frog
P50501	*Rana esculenta*	161	- T*D**RRRH*DVSGSVP	173	edible frog

NCBI website: http://www.ncbi.nlm.nih.gov/blast/.

mutagenesis, and biological assays. Understanding the domains and interactions that regulate AQP channel function may offer new insight into the diversity of functional properties seen in different types of preparations and their contribution to cellular physiology in water-transporting epithelia.

In our model, nucleotide binding to the cytoplasmic side of the channel is suggested to trigger an outward motion of the cytoplasmic D loops that are located at the entrance of the pore. As these loops are juxtapositioned with the CCR, their outward motion could readily be coupled to the opening of the cytoplasmic gate, leading to the partial hydration of the pore. Propagation of the hydration effect and widening of the channel from the cytoplasmic into the periplasmic half of the channel would be needed to complete the hydration and proposed transition to the open state. Confirming specific interactions between cGMP and AQP1 requires more detailed investigations; however, our results suggest that multiple interactions between the nucleotide and the abundant arginine side chains on the cytoplasmic face of AQP1, especially the four consecutive arginines on loop D, could play an important role in nucleotide binding and subsequent gating of the central pore.

Results of our theoretical predictions and biological assays suggest that the ion channel function of AQP1 is sensitive to the amino acid sequence of loop D, which could serve as a direct gate or could interact with other regions of the channel that in turn establish the open ion-channel state. The fact that selective mutation of residues within the AQP1 protein has a substantial effect on ion channel conductance further demonstrates that the cGMP-dependent cationic current is mediated by AQP1. The series of arginines in loop D are highly conserved among AQP1 sequences across species and phyla (Table 1, compiled from the NIH Protein Database), but based on our data showing no impairment of osmotic water permeability, these residues do not seem to be essential for the water-channel function of AQP1. What evolutionary pressure would favor the retention of this loop sequence if the AQP1 channel is nothing but a water channel? One possible explanation is a role for loop D in the regulation of another process, such as ion-channel activity.

The interaction of cGMP with the positively charged arginine residues is intriguing, but whether this loop region serves as part of the direct binding site for ligand-mediated activation cannot be evaluated. Other work has suggested that the carboxyl terminal domain of AQP1 also influences activation of the ionic conductance (Anthony et al., 2000; Boassa and Yool, 2003; Saparov et al., 2001), and it is possible that the activation process involves interactions between multiple cytoplasmic regions of the AQP1 channel. It is conceivable that simultaneous binding of cGMP to its specific binding site, which might be located closer to the periphery of the AQP1 tetramer, and its interaction with the long side chains of the arginine array on loop D could be the mechanism by which the loop is pulled back away from the central pore. Certainly there is a precedent for the contributions of conserved arginine residues as key elements in the binding of cyclic nucleotides in other proteins. For example, in rod photoreceptor cyclic-nucleotide-gated cation channels, an arginine forms an important ionic interaction with the cyclized phosphate of bound cGMP (Tibbs et al., 1998). Nucleotide binding in other proteins also requires interactions with arginines, such as in Cdc42 (a member of the Rho family of GTP binding proteins) (Fidyk and Cerione, 2002), in UCP1 (uncoupling protein in brown adipose tissue) (Echtay et al., 2001), in GAP function (GTPase activating protein) (Vitale et al., 1998), and others.

Mutation of an asparagine (Asn-60) in the anion-conducting channel AQP6 to glycine switches the selectivity of the channel from ions to water, illustrating a capacity for conformational flexibility that was suggested to be unique to AQP6 (Liu et al., 2005). In contrast to the rigid structure commonly envisioned as a general feature of AQPs, data from Liu and colleagues for AQP6 and our data here for AQP1 suggest that these molecules may be more flexible than has been appreciated from the snapshot views provided by crystal structure thus far.

In none of our simulations, did we observe any appreciable change in the monomeric architecture of AQP1. This could be of particular importance for water conduction through the monomeric water pores in AQP1. We were surprised to find that the gating of the central pore could take place without any obvious perturbation

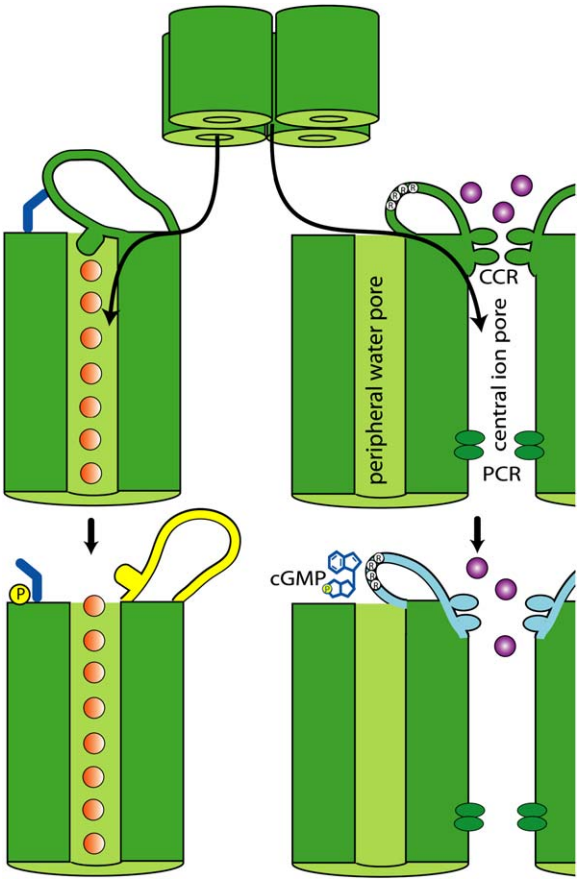

Figure 6. Similarities in the Involvement of Loop D in the Gating of Water Subunit Pores and the Central Pore in Different AQPs

Left, gating of monomeric water pores in a plant AQP. Phosphorylation of a conserved site unleashes the cytoplasmic loop D, which results in opening of the water pore through two complementary mechanisms: displacement of loop D from the pore's entrance and removing the hydrophobic residue blocking the pore (Törnroth-Horsefield et al., 2006). Right, the central pore in mammalian AQP1 also appears to be gated by conformational changes in loop D. In AQP1, loop D is shorter than that in the plant AQP, and a ligand (cGMP) appears to be needed to bridge the link between the loop and unidentified adjacent regions that could hold the loop in the open state.

of the water pores, suggesting that there would be little effect on the constitutive osmotic water permeability of the channel. This observation supports the idea that ion permeation and water permeation through AQP1 are functionally independent of each other, and one can be regulated without affecting the other.

In addition to providing theoretical evidence for the involvement of the putative central pore in ion conductivity, the results of the present work provide for the first time, a plausible mechanism for gating of the central pore in AQPs. Recently, the mechanism of phosphorylation-mediated gating of individual water pores in a plant AQP was reported in a study applying X-ray crystallography and simulation (Törnroth-Horsefield et al., 2006). The similarity between the mechanism proposed in the present work and the one reported by Törnroth-Horsefield et al. (Törnroth-Horsefield et al., 2006) for water pores is striking (Figure 6). In both cases specific hydrophobic residue(s) form a gate in the cytoplasmic half channel that physically blocks the access of the substrate to the channel, thus creating a closed state. These barrier residues in the plant and mammalian AQPs are structurally proximal to and conformationally linked with loop D; in both cases, loop D physically occludes the cytoplasmic entrance of the central pore. The conformational state of this loop, which is controlled by various signaling messages, e.g., cGMP or phosphorylation, might be a broader mechanism within the general family of AQP-related channels that modulates the conformation of gating residues and thus determines whether the channel is in its open state or in a closed state.

Experimental Procedures

Molecular Dynamics Simulations

Monomeric AQP1 was taken from the 2.2 Å resolution structure of bovine AQP1 (Sui et al., 2001) (PDB code: 1J4N). A tetramer with the central pore aligned along the z axis was constructed in VMD (Humphrey et al., 1996) by using the transformation matrices provided in the PDB file and was embedded in a POPE lipid bilayer and solvated by a 15 Å thick slab of water on each side (see Figure 1). Twelve chloride ions were randomly placed into the bulk water in order to neutralize the positive charges of the AQP1 tetramer; the number of chloride ions was adjusted after adding cGMP and/or sodium ions to keep the system electro-neutral. Given the size of the simulation unit cell, the ionic strength of the system is on the order of 100 mM. The system was first equilibrated for 500 ps with the protein fixed under constant temperature (310 K) and constant pressure (1 atm) conditions (NpT ensemble). The protein was then released and another 450 ps of equilibration was performed under the same conditions. All further MD simulations described here were started from the last frame of this equilibration. In one of the subsequent simulations, which is used as the control simulation, the equilibration of the system was continued under the same conditions for additional 3 ns. All simulations were performed with the program NAMD2 (Phillips et al., 2005), the CHARMM27 set of force field parameters (MacKerell et al., 1998), and the TIP3 (Jorgensen et al., 1983) model for water. An integration time step of 1 fs and periodic boundary conditions were applied in all simulations. Van der Waals forces were calculated with a smooth (10–12 Å) cutoff. The Particle Mesh Ewald (PME) method (Essmann et al., 1995) was employed for calculation of full electrostatics, with a grid density of at least 1/Å. The pressure (1 atm) was controlled by the Nosé Hoover Langevin piston method (Feller et al., 1995; Martyna et al., 1994) with an oscillation period of 200 fs and a damping time of 100 fs. A Langevin thermostat (Brünger, 1992) acting on all heavy atoms was used for temperature control (310 K) with a coupling coefficient of 5/ps.

Cation-Induced Conformational Changes of the Pore

The sodium ion was placed at three different locations along the channel axis: (1) in the cytoplasmic half of the pore (z = −6) where side chains of LEU172 and PHE176 form the narrowest part of the pore, which we refer to as the cytoplasmic constriction region; (2) in the middle of the channel (z = 0) corresponding to the midpoint of the lipid bilayer; and (3) in the periplasmic half (z = +6) near the other narrow region of the pore formed by side chains of VAL52 and LEU56 (periplasmic constriction region). The relative position of the ions along the channel axis can be best viewed in Figure 1, where the side view of the tetramer and the z axis are depicted. In each simulation, the motion of the ion along the z axis was constrained by a harmonic potential with a force constant k = 2 kcal/mol·Å^2, and the system was simulated for 10 ns. In addition, two 3 ns simulations with the sodium ion constrained at z = −20 and z = +20, respectively, were performed to detect if the presence of the ion in bulk water near the cytoplasmic or periplasmic vestibules would result in any major protein conformational changes.

Permeation of a Sodium Ion through the Central Pore

Steered molecular dynamics (SMD) (Isralewitz et al., 2001) was employed to induce full ion permeation events by pulling a sodium ion

through the central pore all the way from one side of the membrane to the other side. A harmonic constraint (k = 2 kcal/mol·Å^2) moving at a velocity of v = 0.04 Å/ps was used to pull the ion along the channel axis (z direction). Each pulling simulation took about 1 ns.

Simulating full permeation events provides a complete dynamical picture of how an ion passes through and affects the whole channel. However, since the pulling process is comparatively fast, it may not necessarily trigger stable conformational changes in the channel. To enhance the ion permeation effect on the channel, we performed four successive SMD simulations on the system. In other words, the same pore was used for successive permeations of four ions. In each simulation, an ion was pulled from the cytoplasmic side (at z = −20) to the periplasmic side (at z = +20). Successive simulations were separated by an equilibration phase (~500 ps), during which the ion was constrained to the cytoplasmic side.

SMD simulations applying slower pulling speeds (v = 0.01 Å/ps) were used to reconstruct the potential of mean force (PMF) of ion permeation. The procedure, which followed closely one reported earlier (Jensen et al., 2002), is described in Supplemental Data. After 10 ns of equilibration with a sodium ion at the cytoplasmic constriction region, water entered and partially hydrated the pore, resulting in a configuration that we refer to as the "quasiopen" state. To verify whether the induced hydration has any facilitatory effect on ion conduction, the PMF of ion permeation through this partially hydrated channel was also calculated (details given in Supplemental Data).

Simulations of cGMP Binding

In order to study the effect of cGMP binding to AQP1, four cGMP molecules were placed at the cytoplasmic side of the equilibrated AQP1 system near the perimeter of the tetramer. The initial positions of the cGMP molecules were inferred from the superposition of the crystal structure of a cGMP bound carboxy-terminal fragment of HCN2 (potassium/sodium hyperpolarization-activated cyclic nucleotide-gated channel 2; solved at 1.9 Å, PDB code: 1Q3E) (Zagotta et al., 2003), with the C terminus (residues 229–249; with 250–269 missing) of AQP1, according to their sequence alignment as reported earlier (Anthony et al., 2000; Zagotta et al., 2003). After simulating the system for 500 ps with the protein and the cGMPs constrained in position, nucleotides were released to allow free diffusion, and the simulation continued for another 500 ps, while the Cα atoms of the protein remained constrained. Subsequently, all atoms of the system were freed, and the simulation continued for additional 10 ns, during which significant displacements of cGMP molecules on the cytoplasmic surface of the protein were observed. During the simulations, diffusion of the cGMP molecules and their interactions with the protein were monitored.

Experimental Measurement of Water and Ion Conduction

Oocyte preparation and injection was done as described previously (Anthony et al., 2000). In brief, oocytes of *Xenopus laevis* were treated in collagenase and injected with either 50 nl of water (control oocytes); or 50 nl of water containing 1 ng AQP1 wild-type or 1 ng AQP1 mutant cRNA. Oocytes were maintained at 18°C in ND96 culture medium (96 mM NaCl, 2 mM KCl, 1.8 mM $CaCl_2$, 2.5 mM Na-pyruvate, 5 mM HEPES [pH 7.6]) to allow the expression of AQP1 channels. Wild-type human AQP1 cDNA was provided by Dr. Peter Agre. Site-directed mutations were generated from custom oligonucleotide primers with the Stratagene (La Jolla, CA) Quik-Change kit. The desired mutations in the correct reading frame were confirmed by DNA sequencing. Osmotic swelling was analyzed from volume changes recorded by video camera (Scion Image), initiated with the transfer of AQP1-expressing or control oocytes at time zero into 50% hypotonic saline (NaCl 50 mM, $MgCl_2$ 5 mM, HEPES 5 mM [pH 7.3]). Data were analyzed as the rate of change in volume with time, standardized to the initial volume at time zero.

For two-electrode voltage-clamp recordings, electrodes were filled with 3 M KCl. The recording saline contained 100 mM NaCl, 5 mM $MgCl_2$, and 5 mM HEPES (pH 7.3). After the initial recording, generation of intracellular cGMP was induced by extracellular application of the nitric oxide donor, sodium nitroprusside (SNP), at a final concentration (1–10 mM) adjusted empirically for each batch of oocytes in order to activate the AQP1 channels without background endogenous currents. Recordings were made with a GeneClamp amplifier and pClamp software (Axon Instruments, Foster City, CA).

Supplemental Data

Supplemental Data include a figure showing the hydration of the central pore as a result of successive pullings of a sodium ion and the details of the method used to reconstruct the potentials of mean force from the SMD simulations and are available at http://www.structure.org/cgi/content/full/14/9/1411/DC1/.

Acknowledgments

The present work was supported by grants from the National Institutes of Health P41-RR05969, R01-GM067887, and R01-GM059986. The authors also acknowledge computer time provided at the National Science Foundation centers by the grant NRAC MCA93S028. Molecular images in this paper were generated with the molecular graphics program VMD (Humphrey et al., 1996).

Received: March 10, 2006
Revised: July 11, 2006
Accepted: July 13, 2006
Published: September 12, 2006

References

Abu-Hamdah, R., Cho, W.J., Cho, S.J., Jeremic, A., Kelly, M., Ilie, A.E., and Jena, B.P. (2004). Regulation of the water channel aquaporin-1: isolation and reconstitution of the regulatory complex. Cell Biol. Int. *28*, 7–17.

Agre, P. (2004). Aquaporin water channels (nobel lecture). Angew. Chem. Int. Ed. Engl. *43*, 4278–4290.

Agre, P., Bonhivers, M., and Borgnia, M.J. (1998). The aquaporins, blueprints for cellular plumbing systems. J. Biol. Chem. *273*, 14659–14662.

Agre, P., King, L.S., Yasui, M., Guggino, W.B., Ottersen, O.P., Fujiyoshi, Y., Engel, A., and Nielsen, S. (2002). Aquaporin water channels—from atomic structure to clinical medicine. J. Physiol. *542*, 3–16.

Allen, R., Melchionna, S., and Hansen, J. (2002). Intermittent permeation of cylindrical nanopores by water. Phys. Rev. Lett. *89*, 175502.

Anthony, T., Brooks, H., Boassa, D., Leonov, S., Yanochko, G., Regan, J., and Yool, A. (2000). Cloned human aquaporin-1 is a cyclic GMP-gated ion channel. Mol. Pharmacol. *57*, 576–588.

Beckstein, O., and Sansom, M.S.P. (2003). Liquid-vapor oscillations of water in hydrophobic nanopores. Proc. Natl. Acad. Sci. USA *100*, 7063–7068.

Beckstein, O., and Sansom, M.S. (2004). The influence of geometry, surface character, and flexibility on the permeation of ions and water through biological pores. Phys. Biol. *1*, 42–52.

Beckstein, O., Tai, K., and Sansom, M.S.P. (2004). Not ions alone: barriers to ion permeation in nanopores and channels. J. Am. Chem. Soc. *126*, 14694–14695.

Boassa, D., and Yool, A. (2002). A fascinating tail: cGMP activation of aquaporin-1 ion channels. Trends Pharmacol. Sci. *23*, 558–562.

Boassa, D., and Yool, A. (2003). Single amino acids in the carboxyl terminal domain of aquaporin-1 ion channels contribute to cGMP-dependent activation. BMC Physiol. *3*, 12.

Boassa, D., Stamer, W.D., and Yool, A.J. (2006). Ion channel function of aquaporin-1 natively expressed in choroid plexus. J. Neurosci. 7811–7819.

Bok, D., Dockstader, J., and Horwitz, J. (1982). Immunocytochemical localization of the lens main intrinsic polypeptide (MIP26) in communicating junctions. J. Cell Biol. *92*, 213–220.

Borgnia, M., Nielsen, S., Engel, A., and Agre, P. (1999). Cellular and molecular biology of the aquaporin water channels. Annu. Rev. Biochem. *68*, 425–458.

Brünger, A.T. (1992). X-PLOR, Version 3.1: A System for X-Ray Crystallography and NMR (New Haven, CT: Yale University Press).

Chakrabarti, N., Tajkhorshid, E., Roux, B., and Pomès, R. (2004). Molecular basis of proton blockage in aquaporins. Structure *12*, 65–74.

de Groot, B.L., and Grubmüller, H. (2001). Water permeation across biological membranes: mechanism and dynamics of aquaporin-1 and GlpF. Science *294*, 2353–2357.

de Groot, B.L., Engel, A., and Grubmüller, H. (2001). A refined structure of human aquaporin-1. FEBS Lett. *504*, 206–211.

de Groot, B.L., Frigato, T., Helms, V., and Grubmüller, H. (2003). The mechanism of proton exclusion in the aquaporin-1 water channel. J. Mol. Biol. *333*, 279–293.

Echtay, K., Bienengraeber, M., and Klingenberg, M. (2001). Role of intrahelical arginine residues in functional properties of uncoupling protein (ucp1). Biochemistry *40*, 5243–5248.

Essmann, U., Perera, L., Berkowitz, M.L., Darden, T., Lee, H., and Pedersen, L.G. (1995). A smooth particle mesh Ewald method. J. Chem. Phys. *103*, 8577–8593.

Feller, S.E., Zhang, Y.H., Pastor, R.W., and Brooks, B.R. (1995). Constant pressure molecular dynamics simulation—the Langevin piston method. J. Chem. Phys. *103*, 4613–4621.

Fidyk, N., and Cerione, R. (2002). Understanding the catalytic mechanism of GTPase-activating proteins: demonstration of the importance of switch domain stabilization in the stimulation of GTP hydrolysis. Biochemistry *41*, 15644–15653.

Fu, D., Libson, A., Miercke, L.J.W., Weitzman, C., Nollert, P., Krucinski, J., and Stroud, R.M. (2000). Structure of a glycerol conducting channel and the basis for its selectivity. Science *290*, 481–486.

Gonen, T., Sliz, P., Kistler, J., Cheng, Y., and Walz, T. (2004). Aquaporin-0 membrane junctions reveal the structure of a closed water pore. Nature *429*, 193–197.

Gonen, T., Cheng, Y., Sliz, P., Hiroaki, Y., Fujiyoshi, Y., Harrison, S.C., and Walz, T. (2005). Lipidprotein interactions in double-layered two-dimensional AQP0 crystals. Nature *438*, 633–638.

Grayson, P., Tajkhorshid, E., and Schulten, K. (2003). Mechanisms of selectivity in channels and enzymes studied with interactive molecular dynamics. Biophys. J. *85*, 36–48.

Harries, W.E.C., Akhavan, D., Miercke, L.J.W., Khademi, S., and Stroud, R. (2004). The channel architecture of aquaporin 0 at a 2.2-angstrom resolution. Proc. Natl. Acad. Sci. USA *101*, 14045–14050.

Heymann, J.B., and Engel, A. (1999). Aquaporins: phylogeny, structure, and physiology of water channels. News Physiol. Sci. *14*, 187–193.

Heymann, J.B., Agre, P., and Engel, A. (1998). Progress on the structure and function of aquaporin 1. J. Struct. Biol. *121*, 191–206.

Humphrey, W., Dalke, A., and Schulten, K. (1996). VMD: visual molecular dynamics. J. Mol. Graph. *14*, 33–38.

Ilan, B., Tajkhorshid, E., Schulten, K., and Voth, G.A. (2004). The mechanism of proton exclusion in aquaporin channels. Proteins *55*, 223–228.

Isralewitz, B., Gao, M., and Schulten, K. (2001). Steered molecular dynamics and mechanical functions of proteins. Curr. Opin. Struct. Biol. *11*, 224–230.

Jan, L., and Jan, Y. (1992). Structural elements involved in specific K^+ channel functions. Annu. Rev. Physiol. *54*, 537–555.

Jensen, M.Ø., Tajkhorshid, E., and Schulten, K. (2001). The mechanism of glycerol conduction in aquaglyceroporins. Structure *9*, 1083–1093.

Jensen, M.Ø., Park, S., Tajkhorshid, E., and Schulten, K. (2002). Energetics of glycerol conduction through aquaglyceroporin GlpF. Proc. Natl. Acad. Sci. USA *99*, 6731–6736.

Jensen, M.Ø., Tajkhorshid, E., and Schulten, K. (2003). Electrostatic tuning of permeation and selectivity in aquaporin water channels. Biophys. J. *85*, 2884–2899.

Jorgensen, W.L., Chandrasekhar, J., Madura, J.D., Impey, R.W., and Klein, M.L. (1983). Comparison of simple potential functions for simulating liquid water. J. Chem. Phys. *79*, 926–935.

King, L., and Arge, P. (1996). Pathophysiology of the aquaporin water channels. Annu. Rev. Physiol. *58*, 619–648.

Lee, J.K., Kozono, D., Remis, J., Kitagawa, Y., Agre, P., and Stroud, R. (2005). Structural basis for water conductance by the archaeal aquaporin AqpM. Proc. Natl. Acad. Sci. USA *102*, 18932–18937.

Liu, K., Kozono, D., Kato, Y., Agre, P., and Yasui, A.H.M. (2005). Conversion of aquaporin 6 from an anion channel to a water-selective channel by a single amino acid substitution. Proc. Natl. Acad. Sci. USA *102*, 2192–2197.

MacKerell, A.D., Jr., Bashford, D., Bellott, M., Dunbrack, R.L., Jr., Evanseck, J., Field, M.J., Fischer, S., Gao, J., Guo, H., Ha, S., et al. (1998). All-atom empirical potential for molecular modeling and dynamics studies of proteins. J. Phys. Chem. B *102*, 3586–3616.

Martyna, G.J., Tobias, D.J., and Klein, M.L. (1994). Constant pressure molecular dynamics algorithms. J. Chem. Phys. *101*, 4177–4189.

Murata, K., Mitsuoka, K., Hirai, T., Walz, T., Agre, P., Heymann, J.B., Engel, A., and Fujiyoshi, Y. (2000). Structural determinants of water permeation through aquaporin-1. Nature *407*, 599–605.

Phillips, J.C., Braun, R., Wang, W., Gumbart, J., Tajkhorshid, E., Villa, E., Chipot, C., Skeel, R.D., Kale, L., and Schulten, K. (2005). Scalable molecular dynamics with NAMD. J. Comput. Chem. *26*, 1781–1802.

Pohl, P., Saparov, S.M., Borgnia, M.J., and Agre, P. (2001). Highly selective water channel activity measured by voltage clamp: analysis of planar lipid bilayers reconstituted with purified AqpZ. Proc. Natl. Acad. Sci. USA *98*, 9624–9629.

Preston, G.M., and Agre, P. (1991). Isolation of the cDNA for erythrocyte integral membraneprotein of 28 kilodaltons: member of an ancient channel family. Proc. Natl. Acad. Sci. USA *88*, 11110–11114.

Preston, G.M., Carroll, T.P., Guggino, W.B., and Agre, P. (1992). Appearance of water channels in *Xenopus* oocytes expressing red cell CHIP28 protein. Science *256*, 385–387.

Saparov, S.M., Kozono, D., Rothe, U., Agre, P., and Pohl, P. (2001). Water and ion permeation of aquaporin-1 in planar lipid bilayers. J. Biol. Chem. *276*, 31515–31520.

Saparov, S., Tsunoda, S., and Pohl, P. (2005). Proton exclusion by an aquaglyceroprotein: a voltage clamp study. Biol. Cell. *97*, 545–550.

Savage, D.F., Egea, P.F., Robles-Colmenares, Y., O'Connell, J.D., III, and Stroud, R.M. (2003). Architecture and selectivity in aquaporins: 2.5 Å X-ray structure of aquaporin Z. PLoS Biol. *1*, 334–340.

Smart, O.S., Neduvelil, J.G., Wang, X., Wallace, B.A., and Sansom, M.S.P. (1996). HOLE: a program for the analysis of the pore dimensions of ion channel structural models. J. Mol. Graph. *14*, 354–360.

Sotomayor, M., and Schulten, K. (2004). Molecular dynamics study of gating in the mechanosensitive channel of small conductance MscS. Biophys. J. *87*, 3050–3065.

Sui, H., Han, B.-G., Lee, J.K., Walian, P., and Jap, B.K. (2001). Structural basis of waterspecific transport through the AQP1 water channel. Nature *414*, 872–878.

Tajkhorshid, E., Nollert, P., Jensen, M.Ø., Miercke, L.J.W., O'Connell, J., Stroud, R.M., and Schulten, K. (2002). Control of the selectivity of the aquaporin water channel family by global orientational tuning. Science *296*, 525–530.

Tibbs, G., Liu, D., Leypold, B., and Siegelbaum, S. (1998). A state-independent interaction between ligand and a conserved arginine residue in cyclic nucleotide-gated channels reveals a functional polarity of the cyclic nucleotide binding site. Biol. Chem. *273*, 4497–4505.

Törnroth-Horsefield, S., Wang, Y., Hedfalk, K., Johanson, U., Karlsson, M., Tajkhorshid, E., Neutze, R., and Kjellbom, P. (2006). Structural mechanism of plant aquaporin gating. Nature *439*, 688–694.

Tsunoda, S., Wiesner, B., Lorenz, D., Rosenthal, W., and Pohl, P. (2004). Aquaporin-1, nothing but a water channel. J. Biol. Chem. *279*, 11364–11367.

Vitale, N., Moss, J., and Vaughan, M. (1998). Molecular characterization of the GTPase-activating domain of ADP-ribosylation factor domain protein 1 (ard1). J. Biol. Chem. *273*, 2553–2560.

Wang, Y., Schulten, K., and Tajkhorshid, E. (2005). What makes an aquaporin a glycerol channel: a comparative study of AqpZ and GlpF. Structure *13*, 1107–1118.

Yanochko, G., and Yool, A. (2002). Regulated cationic channel function in *Xenopus* oocytes expressing *Drosophila* big brain. J. Neurosci. *22*, 2530–2540.

Yanochko, G., and Yool, A. (2004). Block by extracellular divalent cations of *Drosophila* big brain channels expressed in *Xenopus* oocytes. Biophys. J. *86*, 1470–1478.

Yasui, M., Hazama, A., Kwon, T.-H., Nielsen, S., Guggino, W.B., and Agre, P. (1999). Rapid gating and anion permeability of an intracellular aquaporin. Nature *402*, 184–187.

Yool, A., and Stamer, W. (2002). Novel roles for aquaporins as gated ion channels. In Molecular Insights into Ion Channel Biology in Health and Disease, *Volume 32*, E.E. Bittar and R.A. Maue, eds. (Amsterdam, The Netherlands: Elsevier Science), pp. 351–379.

Yool, A.J., and Weinstein, A.M. (2002). New roles for old holes: ion channel function in aquaporin-1. News Physiol. Sci. *17*, 68–72.

Yool, A., Stamer, W., and Regan, J. (1996). Forskolin simulation of water and cation permeability in aquaporin 1 water channels. Science *273*, 1216–1218.

Yool, A., Brokl, O.H., Pannabecker, T.L., Dantzler, W.H., and Stamer, W.D. (2002). Tetraethylammonium block of water flux in Aquaporin-1 channels expressed in kidney thin limbs of Henle's loop and a kidney-derived cell line. BMC Physiol. *2*, 4.

Zagotta, W., and Siegelbaum, S. (1996). Structure and function of cyclic nucleotide gate channels. Annu. Rev. Neurosci. *58*, 619–648.

Zagotta, W., Olivier, N., Black, K., Young, E., Olson, R., and Gouaux, J. (2003). Structural basis for modulation and agonist specificity of HCN pacemaker channels. Nature *425*, 200–205.

Zeidel, M.L., Nielsen, S., Smith, B.L., Ambudkar, S.V., Maunsbach, A.B., and Agre, P. (1994). Ultrastructure, pharmacological inhibition, and transport selectivity of aquaporin channel-forming integral protein in proteoliposomes. Biochemistry *33*, 1606–1615.

Zhu, F., Tajkhorshid, E., and Schulten, K. (2001). Molecular dynamics study of aquaporin-water channel in a lipid bilayer. FEBS Lett. *504*, 212–218.

Zhu, F., Tajkhorshid, E., and Schulten, K. (2004). Theory and simulation of water permeation in aquaporin-1. Biophys. J. *86*, 50–57.